Proceedings of the 21st ICSMGE, Vienna, Austria, 14 – 19 June 2026. Pistrol, Adam & Schweiger (eds.)
Published by: ÖGG, Austrian Society for Geomechanics, Salzburg, Austria, ISBN 978-3-9503898-4-5
https://doi.org/10.53243/ICSMGE2026-1955

A decoupled model for static soil-foundation interaction using beam and plate elements as foundation structure and interacting springs to represent the soil

Luis Muciñoz
Master's and Doctoral Program in Engineering, National Autonomous University of Mexico, Mexico City, Mexico, luismucinoz@comunidad.unam.mx

Rigoberto Rivera, Carmelino Zea
Division of Civil Engineering and Geomatics - Faculty of Engineering, National Autonomous University of Mexico, Mexico City, Mexico, riverac@unam.mx, zeaconcar@hotmail.com

Juan Pérez-Gavilán, **Miguel Mánica**
Institute of Engineering, National Autonomous University of Mexico, Mexico City, Mexico, jperezgavilane@iingen.unam.mx, mmanicam@iingen.unam.mx

ABSTRACT: This paper proposes a model for analyzing the static soil-foundation interaction of shallow foundations. The model incorporates thin plate elements and shear-deformable beam elements to represent the foundation structure. The stiffness matrices of both elements, derived from a finite element approach, are combined with a soil stiffness matrix calculated by the well-known basic (Boussinesq, 1885) solution integrated for uniformly distributed loads over polygonal shaped surfaces (Damy J. and Casales C., 1985) and the coefficient of volume compressibility (Terzaghi, 1943) of the underlying soils, providing a suitable basis for describing soil behavior beneath the foundation. The main purpose of this tool is to evaluate the effect of plate elements on soil-foundation interaction, analyzing how these elements influence the overall behavior of the system. On the other hand, the model generates fields of modulus of subgrade reaction, treated as nodal interacting springs that represent the behavior of the underlying soil. The model was implemented in Python, to improve accessibility and efficiency in its application. It is presented as a practical tool for analysis and design in foundation engineering.

KEYWORDS: Soil-foundation interaction, shallow foundations, finite element model, modulus of subgrade reaction, Python implementation.

1 INTRODUCTION

The static Soil-Structure interaction is a fundamental aspect in the analysis and design of foundations, where the structural response is directly influenced by the behavior of the ground on which they are supported or embedded.

Conventional methods of static soil-structure interaction are based on the principle that displacements at the foundation-soil interface must be equal, meaning there is compatibility in the deformations. The calculation procedure for this interaction generally follows these steps: (a) the displacements of the substructure are calculated, (b) the displacements of the foundation soil are calculated, and (c) the compatibility of deformations between the structure and the soil is established (Demeneghi et al., 2016).

This problem has been widely addressed previously in shallow foundations, either directly, by assimilating the stiffness of the foundation structure through the matrix assembly of a reticular set of beams, and subsequently, establishing the compatibility of displacements with soil settlements (Hermosillo et al., 2024) or by adding the stiffness matrix of the foundation structure with the soil stiffness matrix (López-Rincón, Zea-Constantino and Rivera-Constantino, 2011), derived in turn from the Matrix Settlement Equation methodology developed by (Zeevaert, 1980); or by iterative equilibrium of subsoil reactions (Chamecki, 1956) to cite a few examples.

However, despite the fact that the previously mentioned works propose well-founded and rational alternatives to the practical solution of the Soil-Structure Interaction problem of foundation, they are based on an important simplification, which is to consider the shallow foundation as a grid of beams, which completely excludes the mechanical behavior of the plate structural elements, present in the vast majority of shallow foundations (particularly slabs).

In this context, the static interaction model presented in this paper, although based on existing work and hypotheses, has the advantage of not requiring the assimilation of the stiffness of the foundation structure through beams with equivalent properties. In this paper, a coupled assembly is proposed between the stiffness matrices of a beam grid with shear effect, the stiffness matrices for thin plates based on an analytical solution that is part of the present research, and the stiffness matrix of the supporting soil.

2 MODELING OF STRUCTURAL SYSTEM

The slab on grade system is conceived by assimilating it into a rectangular plate finite element mesh, overlaid with a beam grid where all the vertical freedom degrees in each node are supported in a spring that represents the ground response. This avoids assimilating the foundation system as a simple grid of grade beams with equivalent properties.

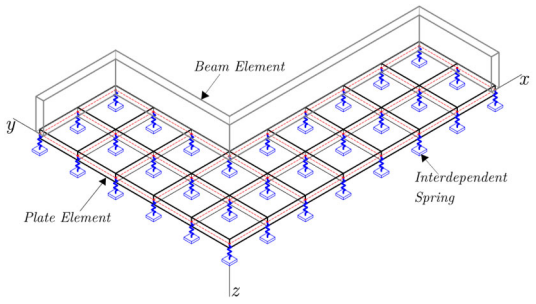

Figure 1. Soil-structure system.

2.1 *Thin plate element*

In order to include the stiffness of the plate elements in the slab on grade and seeking to favor the efficiency and practicality of the model, a finite element solution has been formulated for thin

plates with thickness t, of dimensions a and b aligned with the Cartesian axes $(x: 0 \to a,\ y: 0 \to b)$. Given the nature of the formulation, Kirchhoff's hypotheses have been adopted (Reddy, 2006). Thus, the displacements are defined by:

$$u_\alpha = -z\theta^\alpha, \quad u_3 = w, \quad \theta_x = \frac{\partial w}{\partial y}, \quad \theta_y = -\frac{\partial w}{\partial x} \tag{1}$$

where w is the vertical displacement, which will be approximated by:

$$w = \mathbf{P}^T \mathfrak{A} \tag{2}$$

with:

$$\mathbf{P}^T = \{1\ x\ y\ x^2\ xy\ y^2\ x^3\ x^2y\ xy^2\ y^3\ x^3y\ xy^3\} \tag{3}$$

where $\mathfrak{A}$ is the vector of polynomial coefficients. Then, the nodal conditions at the vertices (w, θ_x, θ_y) state:

$$\mathbf{C}\mathfrak{A} = \tilde{\mathbf{u}} \ \Rightarrow\ \mathfrak{A} = \mathbf{C}^{-1}\tilde{\mathbf{u}} \tag{4}$$

where $\tilde{\mathbf{u}}$ arranges the 12 nodal degrees of freedom.

On the other hand, deformations are related to spatial derivatives through:

$$\varepsilon = -z\mathbf{S}w, \qquad \mathbf{S} = \left\{\frac{\partial^2}{\partial x^2} \quad \frac{\partial^2}{\partial y^2} \quad 2\frac{\partial^2}{\partial x \partial y}\right\}^T \tag{5}$$

Now following Hooke's Law for Plane Stress:

$$\sigma = \mathbf{D}\varepsilon, \qquad \mathbf{D} = \frac{E}{1-\nu^2}\begin{bmatrix} 1 & \nu & 0 \\ \nu & 1 & 0 \\ 0 & 0 & \frac{1-\nu}{2} \end{bmatrix} \tag{6}$$

it is possible to define:

$$\begin{aligned} \sigma = \mathbf{D}\varepsilon = -z\mathbf{D}\mathbf{S}w &= -z\mathbf{D}\mathbf{S}\mathbf{P}^T\mathfrak{A} \\ &= -z\mathbf{D}\mathbf{S}\mathbf{P}^T\mathbf{C}^{-1}\tilde{\mathbf{u}} \\ &= -z\mathbf{D}\mathbf{Q}\mathbf{C}^{-1}\tilde{\mathbf{u}} \end{aligned} \tag{7}$$

where it can be noticed:

$$\varepsilon = -z\mathbf{Q}\mathbf{C}^{-1}\tilde{\mathbf{u}},\ \mathbf{Q} = \mathbf{S}\mathbf{P}^T \tag{8}$$

the deformation energy then becomes:

$$\begin{aligned} &\int_V \sigma^T\varepsilon\ dV = z^2\int_V (\mathbf{Q}\mathbf{C}^{-1}\tilde{\mathbf{u}})^T\mathbf{D}\mathbf{Q}\mathbf{C}^{-1}\,\tilde{\mathbf{u}}\,dV \\ &= z^2\int_V \tilde{\mathbf{u}}^T(\mathbf{C}^{-1})^T\mathbf{Q}^T\mathbf{D}\mathbf{Q}\mathbf{C}^{-1}\,\tilde{\mathbf{u}}\,dV \\ &= z^2\int_V \tilde{\mathbf{u}}^T\mathbf{K}_\mathrm{p}\,\tilde{\mathbf{u}}\,dV \end{aligned} \tag{9}$$

and the work due to the external load:

$$\begin{aligned} \int_A q\,w\,dA &= q\int_A \mathbf{P}^T\mathfrak{A}\,dA \\ &= q\int_A \tilde{\mathbf{u}}^T\left(\mathbf{C}^{-1}\right)^T\mathbf{P}\,dA \end{aligned} \tag{10}$$

By minimizing the potential energy functional and parameterizing the domain with dimensions a and b, the stiffness matrix and load vector take the compact form:

$$\mathbf{K}_\mathrm{p} = (\mathbf{C}^{-1})^T\left(\int_0^b\int_0^a \mathbf{Q}^T\mathbf{D}_\mathrm{p}\mathbf{Q}\ dx\,dy\right)\mathbf{C}^{-1} \tag{11}$$

$$\mathbf{f}_\mathrm{q} = q(\mathbf{C}^{-1})^T\int_0^b\int_0^a \mathbf{P}\ dx\,dy \tag{12}$$

Where $\mathbf{D}_\mathrm{p}$ is simply: $\frac{t^3}{12}\mathbf{D}$.

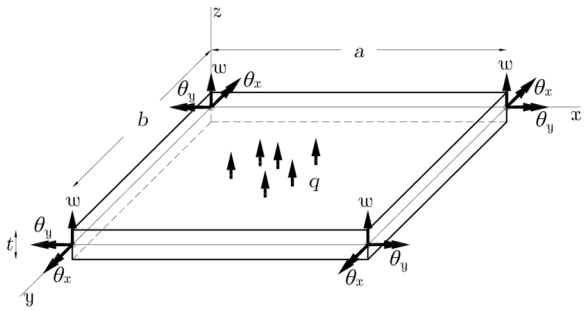

Figure 2. A thin plate finite element.

2.2 *Shear deformable beam element*

Regularly, in slabs on grade, the inclusion of grade beams is required as structural reinforcement.

The shear-deformed beam element implemented in this work follows the finite element formulation proposed by (Fang, 2015), which in turn follows (Timoshenko, 1921) theory. In this formulation, each node has six degrees of freedom: displacements (u, v, w) and rotations $(\theta_x, \theta_y, \theta_z)$, and includes an axis transformation that allows to have beams with any inclination in the xy plane.

3 SOIL RIGIDITY

The determination of ground stiffness using springs is achieved by assuming the soil mass as a continuous medium, discretized into a series of m loaded polygonal areas, where each polygon in turn is assumed to have a constant reaction tributary to each node of the structural system's finite element mesh. That is, each polygonal area represents a nodal spring that assimilates the response of that portion of the domain through a fraction of that area, called the tributary area corresponding to that nodal spring.

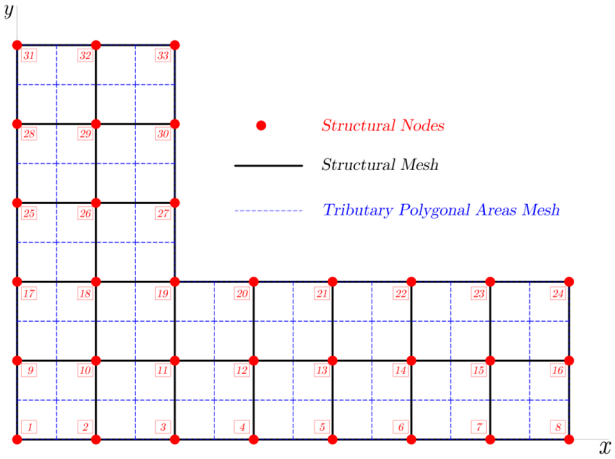

Figure 3. Model of tributary areas to the nodes of the structure

For this purpose, the Settlement Matrix Equation proposed by (Zeevaert, 1980) is used as a starting point.:

$$\delta_j = \overline{\delta}_{ji}q_i \tag{13}$$

Where δ_j is the vertical displacement vector, q_i is the vector of uniformly distributed vertical reactions with area a_i, and $\overline{\delta}_{ji}$ is the vertical displacement matrix. Each of the columns of $\overline{\delta}_{ji}$ is calculated as:

$$\overline{\delta}_{ji} = I_{ji}^N\alpha^N \tag{14}$$

Where I_{ji}^N is the influence matrix generated by the application of a unitary virtual load in each of the tributary area polygons

a_i (Figure 4) computed using the solution for stress distribution in the soil mass under a uniformly loaded polygonal area (Damy J. and Casales C., 1985), and α^N is a vector of compressibility coefficients for the *N* strata considered in the analysis.

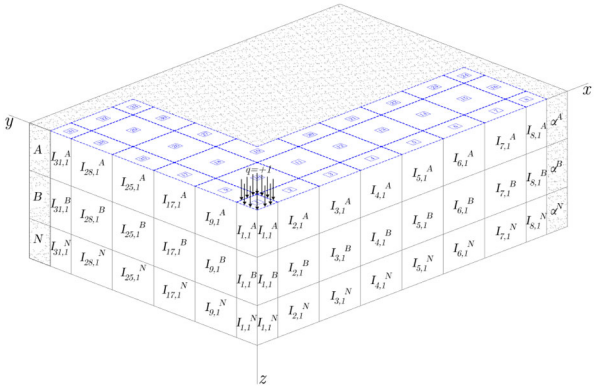

Figure 4. Influences generated by the application of a unitary virtual load.

Thus, by taking the definition for the reaction per unit area $q_i = r_i/a_{(i)}$, it is possible to rewrite (13) as (López-Rincón, Zea-Constantino and Rivera-Constantino, 2011):

$$\delta_j = \overline{\delta}_{ji}\frac{1}{a_{(i)}}r_i = F_{ji}r_i \tag{15}$$

Using matrix notation $\mathbf{F} = \overline{\boldsymbol{\delta}}\mathbf{A}^{-1}$ is the soil flexibility matrix, where $\mathbf{A}$ is a diagonal matrix with a_i as its elements, and $\mathbf{r}$ as the vector of vertical reactions in each polygonal domain.

It can be noticed, that from the expression (15) result:

$$\boldsymbol{\delta} = \mathbf{F}\mathbf{r} \;\Rightarrow\; \mathbf{r} = \mathbf{F}^{-1}\boldsymbol{\delta} = \mathbf{K}_\mathsf{s}\boldsymbol{\delta} \tag{16}$$

where $\mathbf{K}_\mathsf{s}$ is defined as the stiffness matrix of the interdependent system of springs that assimilate and emulate the soil stiffness.

4 SOIL-STRUCTURE INTERACTION ANALYSIS

Since this is a static interaction model, and in order to avoid the need for static condensations to guarantee numerical and structural stability, the system's behavior can be understood through three degrees of freedom (w, θ_x, θ_y).

Firstly, taking the stiffness matrices of the thin plate and beam elements with shear effect, it is possible to generate a coupled matrix of the foundation structure by adding the matrices of both elements. In addition, by reordering the degrees of freedom in the coupled matrix, we have:

$$\mathbf{K}_{\mathsf{fs}} = \mathbf{K}_\mathsf{p} + \mathbf{K}_\mathsf{b} = \begin{bmatrix} \mathbf{k}_{ww} & \mathbf{k}_{w\theta_x} & \mathbf{k}_{w\theta_y} \\ \mathbf{k}_{\theta_x w} & \mathbf{k}_{\theta_x\theta_x} & \mathbf{k}_{\theta_x\theta_y} \\ \mathbf{k}_{\theta_y w} & \mathbf{k}_{\theta_y\theta_x} & \mathbf{k}_{\theta_y\theta_y} \end{bmatrix} \tag{17}$$

The stiffness matrix $\mathbf{K}_{\mathsf{fs}}$ can be assembled with the stiffness matrix of the interdependent spring system $\mathbf{K}_\mathsf{s}$, by adding each component in the vertical displacement degree of freedom w for each node. Thus, by taking advantage of the rearrangement of degrees of freedom, the stiffness matrix of the soil-foundation structure system becomes:

$$\mathbf{K}_{\mathsf{sfs}} = \mathbf{K}_{\mathsf{fs}} + \mathbf{K}_\mathsf{s} = \begin{bmatrix} \mathbf{k}_{ww} + \mathbf{K}_\mathbf{s} & \mathbf{k}_{w\theta_x} & \mathbf{k}_{w\theta_y} \\ \mathbf{k}_{\theta_x w} & \mathbf{k}_{\theta_x\theta_x} & \mathbf{k}_{\theta_x\theta_y} \\ \mathbf{k}_{\theta_y w} & \mathbf{k}_{\theta_y\theta_x} & \mathbf{k}_{\theta_y\theta_y} \end{bmatrix} \tag{18}$$

Then, the force-displacement system of equations, assuming displacement compatibility, can be written as:

$$\begin{Bmatrix} \mathbf{f}_w \\ \mathbf{f}_{\theta_x} \\ \mathbf{f}_{\theta_y} \end{Bmatrix} = \begin{bmatrix} \mathbf{k}_{ww} + \mathbf{K}_\mathbf{s} & \mathbf{k}_{w\theta_x} & \mathbf{k}_{w\theta_y} \\ \mathbf{k}_{\theta_x w} & \mathbf{k}_{\theta_x\theta_x} & \mathbf{k}_{\theta_x\theta_y} \\ \mathbf{k}_{\theta_y w} & \mathbf{k}_{\theta_y\theta_x} & \mathbf{k}_{\theta_y\theta_y} \end{bmatrix} \begin{Bmatrix} \mathbf{d}_w \\ \mathbf{d}_{\theta_x} \\ \mathbf{d}_{\theta_y} \end{Bmatrix} \tag{19}$$

where $\mathbf{d}$ is the coupled vector of nodal displacements and $\mathbf{f}$ the vector of total nodal forces constituted by the sum of the vector of direct nodal forces, the vector of equivalent nodal forces by uniform surface load in the plate elements and the vector of equivalent nodal forces by uniform linear load in the beam elements defined respectively by:

$$\mathbf{f} = \mathbf{f}_\mathsf{n} + \mathbf{f}_\mathsf{q} + \mathbf{f}_\mathsf{e} \tag{20}$$

Once the system has been solved and the nodal displacement vector has been obtained, from equation (13) and the displacement compatibility hypothesis, it is possible to obtain the vector of vertical reactions uniformly distributed in each polygon by:

$$\mathbf{d}_w = \boldsymbol{\delta} = \overline{\boldsymbol{\delta}}\mathbf{q} \Rightarrow \mathbf{q} = \overline{\boldsymbol{\delta}}^{-1}\mathbf{d}_w \tag{21}$$

Similarly, from equation (16) the calculation of the vector of vertical reactions concentrated at the nodes is carried out by means of:

$$\mathbf{d}_w = \boldsymbol{\delta} = \mathbf{F}\mathbf{r} \Rightarrow \mathbf{r} = \mathbf{K}_\mathsf{s}\mathbf{d}_w \tag{22}$$

Thus, the vectors of vertical subgrade reaction modules and Spring Stiffness Constants can be generated by the following component-by-component divisions:

$$k_i = \frac{q_i}{d_{w(i)}}, \qquad K_i = \frac{r_i}{d_{w(i)}} \tag{23}$$

5 PYTHON IMPLEMENTATION

The processes of generation of stiffness matrices for the elements Beam, plate and soil, as well as their assembly and solution in the system of force-displacement equations (Figure 5) were implemented in a series of codes in PYTHON language that allows the export of results and visualization through isovalue maps.

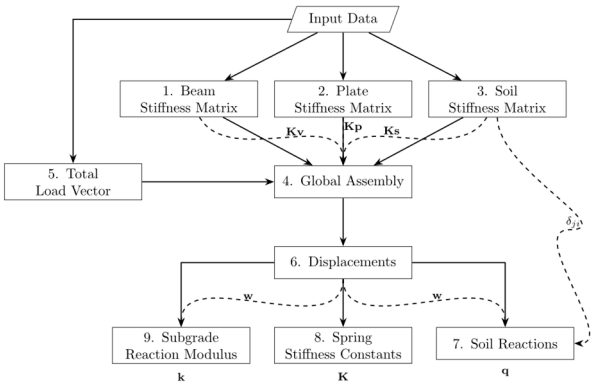

Figure 5. Process diagram of the implementation in Python

6 PRACTICAL EXAMPLE AND COMPARISON

6.1 *Case description*

A real-case study analysis will be performed on a slab on grade supporting a lightweight two-level structure, founded at depth

of 1.5 m in the soft lacustrine clay deposits typical of Mexico City. Since the formulation addressed in this work deals with the interaction problem in a decoupled manner, the reactions at the base of the superstructure were applied as external loads to the foundation structure for analysis. The axial forces are exclusively compressive (-375 to -1100 kN), with overall compressive result of -22009.9 kN. Regarding the bending moments, values of up to ±14.7 kN-m are observed along the longitudinal axis M_x, and between -5.71 kN-m and +11.08 kN-m for M_y. The top view, showing the geometric configuration, as well as the properties of the structural beam and plate elements of the foundation for the analysis, is presented in Figure 6:

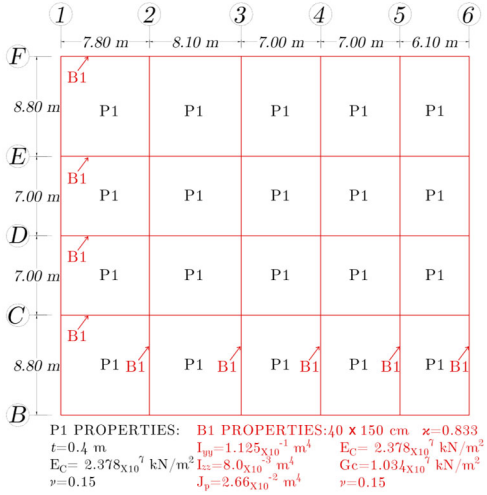

Figure 6. Top view of the foundation configuration

The meshes generated for both the modeling of the plate elements and the tributary areas are of the order of 30 cm per side for each element, this coming from a convergence analysis that guarantees adequate precision in the results.

The stratigraphic characteristics, as well as the mechanical properties associated with the field stress level to which the geotechnical units are subjected, are described in Table 1:

Table 1. Stratigraphy and mechanical properties of the site

GU	Depth (m)	USCS	m_v (m^2/kN)	E_{oed} (kN/ m^2)	ν'
1	0.00-1.50	Fill	0.0000838	11932.20	0.32
2	1.50-4.50	ML	0.0001761	5679.99	0.25
3	4.50-9.00	CH	0.0001317	7595.42	0.30
4	9.00-14.40	CH	0.0003305	3026.15	0.30
5	14.40-21.00	CH	0.0025982	384.89	0.30
6	21.00-23.40	CH	0.0000996	10040.06	0.30
7	23.40-28.80	CH	0.0001016	9844.60	0.30
8	28.80-34.00	CH	0.0000548	18233.20	0.30
9	34.00-37.50	ML	0.0000445	22449.22	0.33
10	37.50-48.50	CH	0.0003830	2611.21	0.30

6.2 *Results comparison*

Based on the characteristics of the case study, an analysis was executed with the codes generated in PYTHON and an analysis of a twin model in the PLAXIS 3D® Finite Element Numerical Modeling platform. For the reproduction of the model in PLAXIS 3D®, a mesh with a Gauss point density analogous to the mesh generated for the analysis in the PYTHON codes, and a Linear Elastic equivalent model was considered (Figure 7).

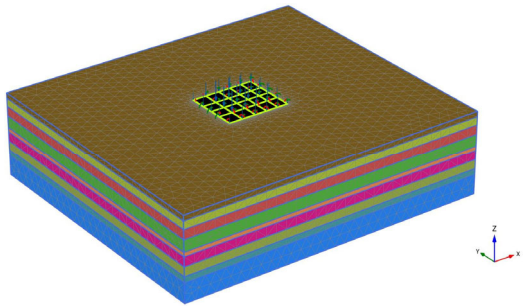

Figure 7. Three-dimensional model in PLAXIS 3D®

Furthermore, in the case of the analysis with the PYTHON codes, it was decided to carry out a refinement in the thicknesses of the original strata underlying the foundation in order to better capture the rapid variation of vertical stresses with depth, inherent with the use of a continuous solution for the determination of soil stiffness matrix.

The displacement results manifested by both models are:

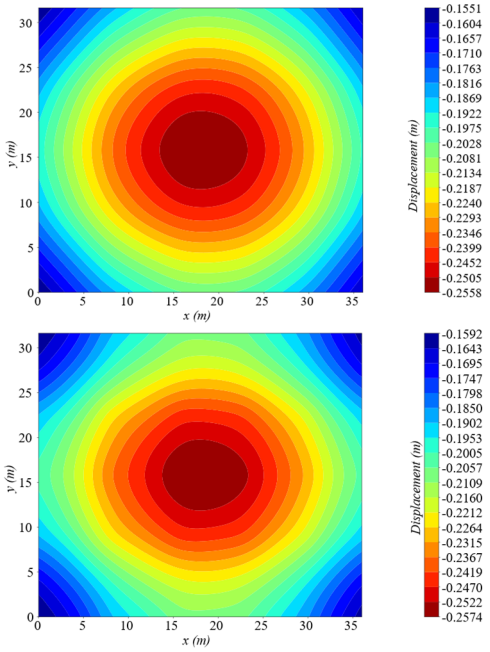

Figure 8. Spatial displacement distribution: (top) results from the developed numerical code; (bottom) results obtained with PLAXIS 3D.

By isolating a vertical axis located at the center of the span formed by axes 3-4 of the foundation, the deformed configuration is:

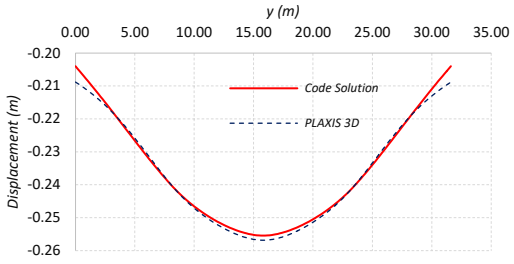

Figure 9. Displacement profile Code Solution-PLAXIS 3D

Here, it can be seen that the displacement profile presents a very similar parabolic geometry in both models, showing maximum differences of the order of 6 mm on the edges, in total displacements that range from 20 to 26 cm, leading to differences of 2 to 3%.

Similarly, the reaction profile on the same vertical axis:

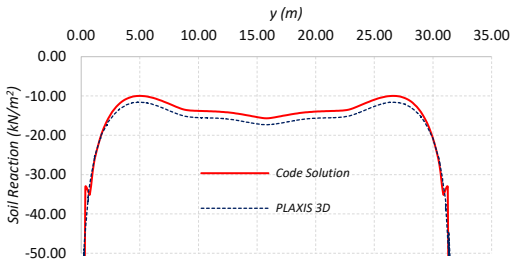

Figure 10. Reaction profile Code Solution-PLAXIS 3D

It is possible to notice that the distribution of soil reactions presents a homogeneous behavior in the central zone of the foundation, but shows an exponential increase in the corners and edges, which is justified under the premise that the use of continuous solutions (such as the one used in the determination of the soil stiffness matrix in this work) leads to infinite contact pressures (reactions) at the edges (Schultze, 1961). Based on this, by clipping the areas close to the edges of the foundation to a maximum value of 50 kN/m^2, the spatial distribution of reactions for both models is:

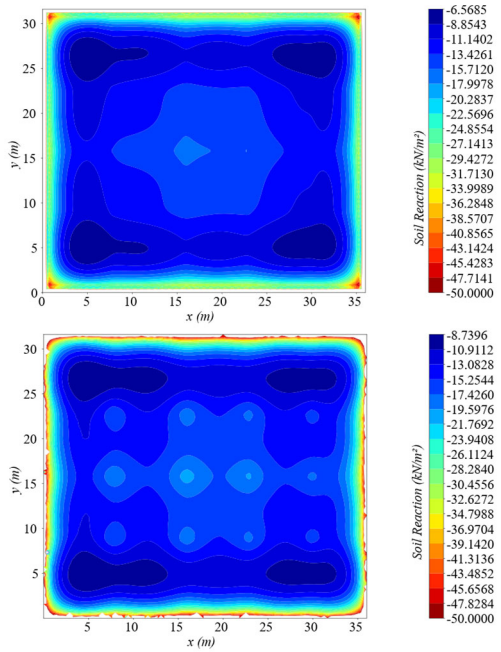

Figure 11. Spatial distribution of soil reactions: (top) results obtained from the implemented numerical code; (bottom) results from PLAXIS 3D.

Given the clear similarity between the results, it was pertinent to obtain both the reaction moduli and the spring stiffness constants using the proposed formulation and the associated results, which can be incorporated into a structural model to emulate the soil response in a decoupled manner. Thus, the spatial distribution of these variables, adopting the same philosophy of clipping the values near the model's edges and corners, are shown in Figure 12:

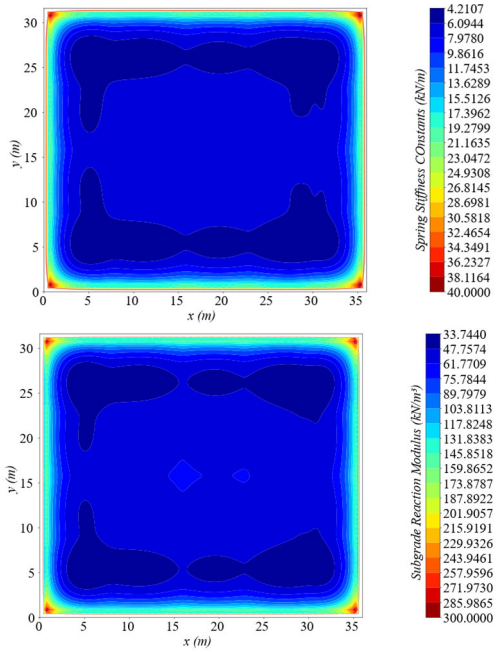

Figure 12. Spatial distribution of (top) spring stiffness constants and (bottom) subgrade reaction modulus.

6.3 *Plate effect*

To compare the effects of the formulation developed in this work, which includes the joint interaction of beam and plate elements, against a model that does not explicitly include the effect of plate elements and uses only a grid of grade beams with equivalent properties, an additional analysis of the same model discussed in the previous section is performed. The difference is that the stiffness provided by the plate elements has been completely excluded, and the beam properties have been modified to equivalent properties.

To this end, it was decided to use the criterion presented in (318 ACI Committee, 2025) and based on the dimensions of the rectangular beams of the original model to calculate the equivalent properties of the grid as inverted T-beams with an effective overhanging flange width on one or both sides of the web, depending on whether it is a central beam or an edge beam in the foundation.

The distribution of displacements for this analysis case is then:

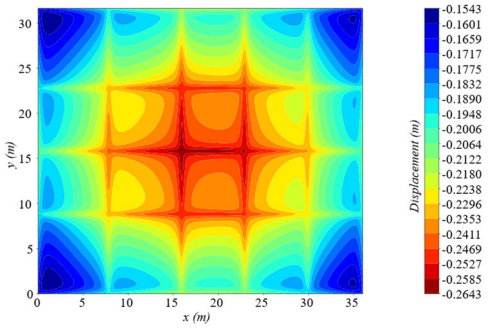

Figure 13. Spatial displacement distribution (only beams)

Now for this case, isolating the vertical axis 3 of the foundation, the comparison of the displacement profiles for the results for both the model with beams and plates, and for the model only with beams of equivalent properties:

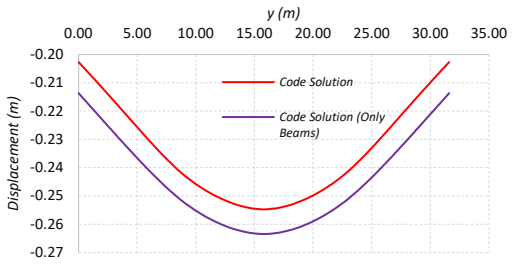

Figure 14. Displacement profile Complete Model-Only Beams

It can be observed that the model incorporating only beams with equivalent properties overestimates displacements by around 1 cm uniformly along the entire axis analyzed. However, despite this overestimation, the difference between the displacements and the model with beams and slabs for this axis is around 5% to 6%.

On the other hand, the soil reaction profile on the same vertical axis:

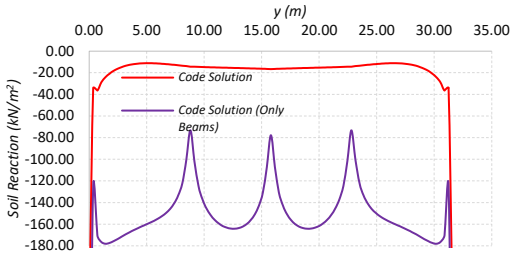

Figure 15. Reaction profile Complete Model-Only Beams

Unlike the displacement comparison, in this case it is clear that the model incorporating only beams with equivalent properties results in a distribution of soil reactions that differs completely from the model explicitly incorporating beams and plates. While the beam-and-plate solution reflects a very uniform distribution in the central region of the axis, the solution incorporating only beams shows a concentration of reactions between the spans, reflecting a localized distribution of stiffness.

7 CONCLUSIONS

The similarity observed between the models, both in the displacement distribution maps and profiles, and in the reactions, suggests that the formulation proposed in this work faithfully reproduces the response patterns for the foundation analyzed. The agreement obtained with the results of the reference numerical model (PLAXIS 3D®) indicates that the developed implementation is suitable for modeling problems under similar conditions.

Excluding plate elements overestimates displacements by 5-6%. This indicates that, for practical purposes, including foundation stiffness under this consideration approximates the results reasonably well in terms of displacement, without the need to incorporate plate elements.

Although the beam-only solution captures a general trend in load transfer, its use could lead to errors in decoupled models where the stiffness of the soil spring system is to be incorporated separately, given that the nature of the model tends to localize and concentrate stiffness only in the axes where beams exist, completely neglecting the effect of spans. This comparison demonstrates the importance of explicitly modeling plate elements when seeking an adequate and accurate estimate of soil reactions and stiffness, even if the displacements can be reasonably well approximated by simplified models.

8 ACKNOWLEDGEMENTS

The authors express their gratitude to the Master's and Doctoral Program in Engineering, the Division of Civil Engineering and Geomatics-Faculty of Engineering, and the Institute of Engineering of the National Autonomous University of Mexico (UNAM) as well as to the Ministry of Science, Humanities, Technology, and Innovation (SECIHTI) for the facilities, institutional support and resources provided during the development of this work.

9 REFERENCES

318 ACI Committee, 2025. ACI CODE-318-25: Building Code for Structural Concrete—Code Requirements and Commentary (ACI CODE-318-25). Technical Documents. Michigan: American Concrete Institute.

Boussinesq, J., 1885. Application des potentiels à l'étude de l'équilibre et du mouvement des solides élastiques: principalement au calcul des deformations et des pressions que produisent, dans ces solides, des efforts quelconques exercés sur und petite partie de leur surface ou de leur intérieur; memoire suivi de notes étendues sur divers points de physique mathématique et d'analyse. Paris: Gauthier-Villars.

Chamecki, S., 1956. Structural Rigidity in Calculating Settlements. Journal of the Soil Mechanics and Foundations Division, 82(1). https://doi.org/10.1061/jsfeaq.0000002.

Damy J. and Casales C., 1985. Soil stresses under a polygonal area uniformly loaded. In: 11th International Conference on Soil Mechanics and Foundation Engineering (San Francisco). [online] San Francisco: International Society for Soil Mechanics and Geotechnical Engineering. pp.733–735. Available at: <https://www.issmge.org/publications/publication/soil-stresses-under-a-polygonal-area-uniformly-loaded> [Accessed 5 May 2025].

Demeneghi, A., Avilés López, J., López Rincón, G., Pérez Rocha, L.E., Sánchez Sesma, J.F., Suárez López, M.M. and Trigos Suárez, J.L., 2016. Interacción Suelo-Estructura, Estática y Dinámica. México: Sociedad Mexicana de ingeniería Geotécnica, A.C.

Fang, W., 2015. EN234: Three-dimentional Timoshenko beam element undergoing axial, torsional and bending deformations. [online] Available at: <https://www.brown.edu/Departments/Engineering/Courses/En2340/Projects/Projects_2015/Wenqiang_Fan.pdf> [Accessed 16 May 2025].

Hermosillo, A., Demeneghi, A., Legorreta, N., Elizalde Enrique, Sanginés Héctor, Guzmán Héctor and Umaña Juan, 2024. Interacción suelo estructura estática de un edificio con cimentación mixta desplantado en suelo friccionante. In: López Acosta Norma Patricia and Espinosa Santiago Alejandra Liliana, eds. XXXII Reunión Nacional de Ingeniería Geotécnica. MEXICO: Sociedad Mexicana de ingeniería Geotécnica, A.C. pp.497–503.

López-Rincón, G., Zea-Constantino, C. and Rivera-Constantino, R., 2011. Una solución directa al problema de interacción suelo-estructura. 2011 Pan-Am CGS Geotechnical Conference.

Reddy, J.N., 2006. Theory and Analysis of Elastic Plates and Shells, Second Edition. Theory and Analysis of Elastic Plates and Shells, Second Edition. https://doi.org/10.1201/9780849384165.

Schultze, E., 1961. Distribution of Stress Beneath a Rigid Foundation. In: Dunod, ed. 5th International Conference on Soil Mechanics and Foundation Engineering (Paris). [online] Paris. p.807. Available at: <https://www.issmge.org/uploads/publications/1/40/1961_01_0134.pdf> [Accessed 10 June 2025].

Terzaghi, K., 1943. Theoretical Soil Mechanics. Theoretical Soil Mechanics. https://doi.org/10.1002/9780470172766.

Timoshenko, S.P., 1921. LXVI. On the correction for shear of the differential equation for transverse vibrations of prismatic bars . The London, Edinburgh, and Dublin Philosophical Magazine and Journal of Science, 41(245). https://doi.org/10.1080/14786442108636264.

Zeevaert, L., 1980. Interacción suelo-estructura de cimentación. Editorial limusa Mexico, .